JAN 1986
RECEIVED
NASA STI FACILITY
ACCESS DEPT.

Dyanmics Explorer Guest Investigator

Final Report for

NASA Research Grant NAG 5-455

Principal Investigator

J. J. Sojka

Utah State University

Center for Atmospheric and Space Sciences

Logan, Utah 84322-3400

Reporting Period

August 1, 1984 to October 31, 1985

Table of Contents

1. Review of Research Actions

The major research goals, that of using Dynamics Explorer (DE) data sets to model the auroral inputs for the Time Dependent Ionospheric Model (TDIM) were achieved. This modelling required DE-1 SAI images and simultaneous DE-2 LAPI particle data. These data sets enabled the large scale relative auroral variations as well as local absolute energy fluxes and characteristic energies to be defined. Our initial storm study period was November 25, 1981, (day 329) from 0300 to 0600 UT. The images enabled global scale auroral modelling with 12 min. time resolution during this period, while the LAPI data enabled a detailed energy flux and characteristic energy calibration of the image model to be made. This auroral model has been used as an input to the TDIM and an ionospheric storm study was carried out.

The only significant problem encountered during the research period was that the image data was not available in digital form until August, 1985. Hence, the main objectives of the study were met but the follow-up goals are still being pursued.

In Appendix 1, the summary from the proposal is reproduced since it listed the original research goals. The data acquisition and determination of inputs to the TDIM, items a) through d) were basically met. The difficulty in getting image data early in the project resulted in our initial study being for a shorter time interval than hoped for. This shorter storm period was for mixed north-south IMF. Because of the convection electric field problem associated with northward IMF conditions, an additional IMF dependent convection model study was carried out. The TDIM results were contrasted with a second storm run using the empirical Spiro et al., 1981, auroral oval model in place

of the image model. Contrasting these two TDIM outputs leads to the goals in item 1) of Appendix 1. Item 2) in the Appendix 1 is still to be carried out, while item 3) is an on-going effort for which a second DE data set will be used as a case study.

2. SAI Image Conversion Algorithm

Theoretical models of the high latitude ionosphere require a representation of the ionization rates associated with auroral particle precipitation. By using SAI images taken at two wavelengths, i.e., 6300 and 5577 $\overset{o}{A}$, it is possible to infer these ionization rates on a global scale. A three step procedure has been developed at USU to obtain these ionization rates. For F-region studies it is critical to use a wavelength (6300 $\overset{o}{A}$) that is sensitive to low energy auroral precipitation; i.e., ionization from < 500 eV electrons results in significant plasma production in the F-region.

The first step is to convert the images to a geographic, and subsequently, to a magnetic reference frame. In this frame, it is possible to define the terminator location as well as the auroral region of interest. At present, the use of near winter solstice data ensures that the auroral oval is almost completely separate from the solar part of the image. Indeed, the use of 6300 and 5577 $\overset{o}{A}$ images is heavily biased towards winter solstice data sets because in sunlight the auroral 6300 and 5577 $\overset{o}{A}$ emissions are swamped and the photometers are saturated. The auroral pixel count rates are converted to kilo Rayleigh intensities, and algorithms have been developed to interpolate over the whole auroral oval. Since the study is focused on global signatures, the problem of emission altitude profile and slant range convection are minimized by using data taken near apogee. These specific problems and that of

updating the Rees and Luckey [1974] work (see below) are currently being tackled by another guest investigator, Dr. Rees.

The second step is to convert auroral emissions to auroral precipitation characteristics. Using the absolute intensity at 5577 $\overset{o}{A}$ as well as the intensity ratio 6300 $\overset{o}{A}$/5577 $\overset{o}{A}$ an algorithm has been developed to produce the corresponding auroral energy flux and characteristic energy. This algorithm is based on the modelling work of Rees and Luckey [1974]. Figure 1 shows graphically the energy flux algorithm; for any combination of intensities at 5577 and 6300 $\overset{o}{A}$ a unique value of the energy flux is obtained. A similar algorithm yields the value of the characteristic energy of the precipitation electrons. The Rees and Luckey model is based on a Maxwellian distribution, hence the characteristic energy is the temperature of a Maxwellian population. The validity of this assumption can be questioned. However, the use of even this zeroth-order approximation is to yield a new method of inferring a basic ionospheric input parameter to an order of precision never before obtainable on a global scale.

The third stage of the procedure is to use the energy flux and characteristic energy of the precipitating particles to compute altitude profiles of the ionization rate for the ions N_2^+, O_2^+, and O^+. This computation is non-trivial, see for example the extensive model of Banks et al. [1974]. At this stage of carrying out a zeroth-order global study the computation of the ionization is significantly simplified. Knudsen et al. [1977] present ionization profiles for N_2^+, O_2^+, and O^+, for two different auroral precipitating spectra. The softer spectrum is for a characteristic energy of ~ 0.2 keV with an energy flux of 0.2 erg/(cm^2s str), while the harder spectrum has a characteristic energy of 2 keV and an energy flux of 0.92 erg/(cm^2s str). These two

sets of ionization profiles are combined by a linear superposition whose ratio is dependent upon the auroral characteristic energy flux obtained from the SAI image analysis. The absolute ionization rate is obtained by scaling this composite ionization profile with the energy flux obtained from the SAI image analysis.

3. Day 329, 1981 Auroral Ionization Model

Our initial test sequence of images are from day 329, 1981 from 0120 to 0609 UT. Images at 6300 and 5577 $\overset{o}{A}$ were available between 0300 and 0600 UT. This sequence was selected because of the marked contrast in 6300 to 5577 $\overset{o}{A}$ around the auroral oval. Plate 1a and 1b show this sequence of images at 6300 and 5577 $\overset{o}{A}$, respectively. These images are in the Iowa "quick look" format. However, they do show how the cusp region is relatively brighter in 6300 $\overset{o}{A}$, while the midnight oval is brighter at 5577 $\overset{o}{A}$. The cusp region becomes bright after ~ 0400 UT, the 6300 images prior to this time do not show the strong cusp emissions. At a time just prior to 0400 UT, the IMF reversed from southward to northward with the northward orientation being maintained for the duration of the images shown in Plate 1.

The image conversion algorithm described in the previous section was applied to each of the images in Plate 1. Then the corresponding pairs of images result in corresponding auroral energy flux and characteristic energy "images". Plate 2a and 2b show these auroral energy flux and characteristic energy images, respectively. These parameters are now plotted in a Magnetic Local Time (MLT) and magnetic latitude polar plot. Each image has the corresponding UT time identified, and the edge of the black circle corresponds to 50° magnetic latitude. For each dial, local noon is at the top and dawn is on

the right. In Plate 2b the wide cusp sector from 0354 UT onwards show very low (< 500 eV) characteristic energy precipitation, this contrasts sharply with the images at 0317 and 0329 where relatively high energy (> 1000 eV) precipitation is present. Images 0430, 0442, and 0452 UT indicate the possible presence of a "theta" type aurora. This would be consistent with the IMF having turned and maintained a strongly northward orientation.

To carry out a calibration or a check of these intensities and characteristic energies, we have used data from Dr. Winningham's LAPI experiment. Figure 2 shows an energy flux comparison of the simultaneous LAPI data and that inferred from the images for this data set. An analysis routine has been developed to plot the image energy flux along the DE-2 satellite track. The left panel of Figure 4 shows the DE-2 satellite track superimposed upon the corresponding 5577 $\overset{\circ}{A}$ auroral image outline. At this time the image absolute calibration is being finalized at Iowa and the comparison shown in Figure 4 is intended to indicate qualitatively our analysis capability. Surprisingly, the third energy flux plot, that from the Spiro et al. [1981] empirical model agrees perfectly with the LAPI data.

Plate 3 shows how the images in Plate 2 are combined to produce auroral ionization rates. For each ion O^+, O_2^+, and N_2^+ the ionization rates are shown at 120, 200, and 300 km in Plate 3. O^+ shows more ionization at 300 than at 200 km. In contrast, the molecular ionization rates decrease with altitude. This contrast is especially marked in the cusp sector where strong fluxes of soft precipitation are present.

4. Ionosphere's Response to Auroral Dynamics

The ionosphere's response time to changes in the ionization rate varies from a few seconds at low altitudes (below 160 km) to several hours (above 500 km) [Sojka and Schunk, 1983]. Thus, the F-region's density variations will be significantly decoupled from the changing auroral conditions as observed by DE SAI images. Using the previously described SAI auroral ionization model, we studied how both the temporal and spatial changes affect the F-region. Figure 3 shows a selected test plasma convection trajectory in a magnetic latitude MLT frame. The contour of energy flux for the image at 0410 UT are superimposed upon the trajectory. Small circle marks along the trajectory indicate every tenth point at which computed TDIM density profiles have been stored. In order to show how the TDIM responds to different images, we have carried out some initial test runs of this trajectory with the image being held fixed for each run. By comparing how the density varies for each run, a means of comparing the images in terms of ionospheric response is obtained.

Plate 4 shows four sets of trajectory-auroral image runs. For each of the runs the electron density as a function of trajectory step and altitude are color coded. The coding is such that dark blue represents densities of 10^3 cm^{-3} and red densities approaching 10^6 cm^{-3}; a dynamic range of 10^3. In addition, a panel shows how the energy flux (SEFLUX) and characteristic energy (EO) inferred from the auroral images varies along the trajectory. The red graph represents the characteristic energy (EO). Panel a in Plate 4 is a reference trajectory run in which no auroral ionization is present; the density variations present are due entirely to solar EUV charges as the plasma convects into and out of sunlight. The trajectory starts at local noon at 69° and at 0000UT and is then followed around two complete times in order that the

magnitude of the TDIM UT effect can be seen. Most of the changes in Panel $\underline{a}$ are smooth, although near step 100 a sharp change occurs, which is a result of the electron temperature and neutral wind changing from sunlit to dark values at the terminator. Panels $\underline{b}$, $\underline{c}$, and $\underline{d}$ correspond to images at 0305, 0442, and 0329 UT, respectively. These three images are quite different from each other as well as from the reference run, Panel $\underline{a}$. Under the winter solstice conditions used, the F-region polar cap and auroral regions are dominated by ionization from auroral precipitation. Image 1, 0305 UT, shown in Panel $\underline{b}$ is the most intense and almost covers the whole test trajectory. Its characteristic energy is also high in the few keV range. The ionosphere responds to this precipitation with an N_mF_2 of $\gtrsim 10^6$ cm^{-3}. In sharp contrast, image 5, 0329 UT, shown in Panel $\underline{d}$ is significantly less intense and, over large sections of the trajectory, no precipitation is present. As a result the N_mF_2 is highly variable ranging from 10^5 to $\sim 6 \times 10^5$ cm^{-3}. The characteristic energy in image 5 ranges from 1 to 2 keV. Image 3, 0442 UT, shown in Panel $\underline{c}$ has characteristic energies which drop below 1 keV to about 500 eV. Indeed, between steps 25 and 60 the characteristic energy increases from ~ 500 eV to 2 keV. During this time, the bottom side of the F-region is seen to drop to lower altitudes as EO increases. Unfortunately, this apparently simple expected correlation is complicated by the fact that SEFLUX is also increasing, which leads to an increasing N_mF_2 and consequently a drop in the bottom side. Plate 4 quantitatively demonstrates how critically the high latitude F-region depends upon the auroral precipitation pattern. The three images used in Plate 4 cover a period of 2 hours, while the test trajectory takes over 10 hours to circulate. Hence, the structure associated with each image in Plate 4 is further complicated by the fact that the temporal auroral changes will introduce another major set of structures. This temporal and spatial depen-

dence can only be incorporated with the data from the DE-SAI experiment. Dynamic TDIM runs using the temporal SAI sequence of images together with the SAI and LAPI analysis carried out in the previous three sections are being prepared for publication.

5. IMF Dependent Convection Model

One of the major new findings of the DE project was the identification of the auroral dynamics associated with "theta" aurora by the SAI imager. Associated with the auroral pattern is an apparent four cell convection pattern with the plasma convecting sunward in the bar in the "theta" shape. Various qualitative models have been suggested to describe how changing IMF conditions cause the ionospheric convection pattern to change [Lyons, 1985; Reiff and Burch, 1985]. In order to carry out model simulation of the high latitude ionosphere's response to such IMF dependences, a multicell convection model is required. We have developed a quantitative mathematical model to describe the IMF dependence. A preprint of a paper describing this model is attached. The DE convection observations will be used to determine how this convection model should vary in a time dependent manner as well as to optimize the model parameters.

REFERENCES

Banks, P. M., C. R. Chappell, and A. F. Nagy, A new model for the interaction of auroral electrons with the atmosphere: Special degradation, backscatter, optical emission, and ionization, J. Geophys. Res., 79, 1459-1470, 1974.

Knudsen, W. C., P. M. Banks, J. D. Winningham, and D. M. Klumpar, Numerical model of the convecting F_2 ionosphere at high-latitudes, J. Geophys. Res., 82, 4784, 1977.

Lyons, L. R., A simple model for polar cap convection patterns and generation of θ auroras, J. Geophys. Res., 90, 1561-1567, 1985.

Rees, M. H. and D. Luckey, Auroral electron energy derived from ratio of spectroscopic emissions, 1. Model computations, J. Geophys. Res., 79, 5181, 1974.

Reiff, P. H. and J. L. Burch, IMF B-dependent plasma flow and Birkeland currents in the dayside magnetosphere 2, A global model for northward and southward IMF, J. Geophys. Res., 90, 1595, 1985.

Sojka, J. J. and R. W. Schunk, A theoretical study of the high latitude F region's response to magnetospheric storm inputs, J. Geophys. Res., 88, 2112-2122, 1983.

Spiro, R. W., P. H. Reiff and L. J. Maher, Precipitating electron energy flux and auroral zone conductances - An empirical model, J. Geophys. Res., 86, 2261, 1981.

APPENDIX 1

Summary from original Proposal

In this proposal, we have described how the DE data could produce unique new inputs for our Time Dependent Ionospheric Model (TDIM). The consequent results from our model would enable us to determine the ionospheric response to realistic dynamic auroral conditions. In addition, the model results can also be used in a "feedback" sense to compare with other DE data sets. We would use the following DE data sets to develop the inputs to our TDIM:

(a) A sequence of auroral images extending up to 36 hours (one hemisphere) from Dr. L. A. Frank's imager would be used to model the dynamics of a magnetospheric storm. The selection of this data set, the empirical modelling, and subsequent conversion from emission rates to precipitation energy fluxes would be a major aspect of the proposed study.

(b) Corresponding precipitation energy fluxes measured by Dr. J. Winningham's LAPI detector on the DE-2 satellite would be used to produce in-situ calibrations to convert the imager emission rates to precipitation energy fluxes.

(c) A semi-empirical magnetospheric convection model (i.e., Volland-Heppner of Heelis-Hanson) will be used as a TDIM input. However, the DE-2 plasma velocity data would be used to determine the best parameters for the model. These data would come from Dr. N. Maynard's VEFI, Dr. R. Heelis' IDM, and Dr. W. Hanson's RPA instruments on DE-2.

(d) The MSIS neutral atmosphere and an elementary high latitude thermospheric wind system are inputs to the TDIM. Data from Dr. G. Carignan's

NACS, Dr. N. Spencer's WATS, and Dr. P. Hays' FPI would be used to check the validity of these inputs or to modify them if needed.

Once these inputs are available our TDIM would be run to produce a model ionosphere with plasma densities for n_e, O^+, NO^+, O_2^+, N_2^+, N^+, and He^+ and the electron and ion temperatures of 4 km altitude intervals from 120 to 800 km over the whole high-latitude region (poleward of 42° magnetic latitude) as a function of time. These results would then be used to:

(1) Investigate the large-scale ionospheric density, composition and temperature responses to realistic magnetospheric auroral inputs. This alone will produce new quantitative knowledge concerning ionosphere-magnetosphere coupling, an objective possible only due to the DE imager and complementary low altitude plasma convection and thermospheric observations.

(2) The computed parameters can be checked with the extensive plasma ion and electron observations made by Dr. L. Brace's LANG and Dr. W. Hanson's RPA on the DE-2 satellite. This will not only lend credence to the modelling, but more importantly, would lead to a better understanding of ionospheric processes.

(3) Having produced a realistic representation of the ionosphere on a global scale we would be in a position to interact with the DE thermospheric efforts already underway, namely the large-scale thermospheric composition and wind modelling being conducted by Dr. R. Roble with his NCAR-TGCM. Our TDIM results would provide a significantly better representation of the ionosphere for his TGCM. In addition, the resulting neutral wind/composition calculations would provide an improved input to

our TDIM. With an iterative procedure we could, for the first time, do a self-consistent study of dynamic thermosphere-ionosphere coupling.

For an initial one-year study period, only one magnetic storm will be focused upon. It is important that the selected storm be representative of an average storm rather than a special case storm. The investigation will concentrate on obtaining all of the model inputs listed above (items a-d). Since the TDIM already exists the remaining efforts will be used to meet items (1) and (2) above. Item (3), that of carrying out thermospheric-ionospheric model interactions, would be pursued at some later stage as would studies of other storm cases.
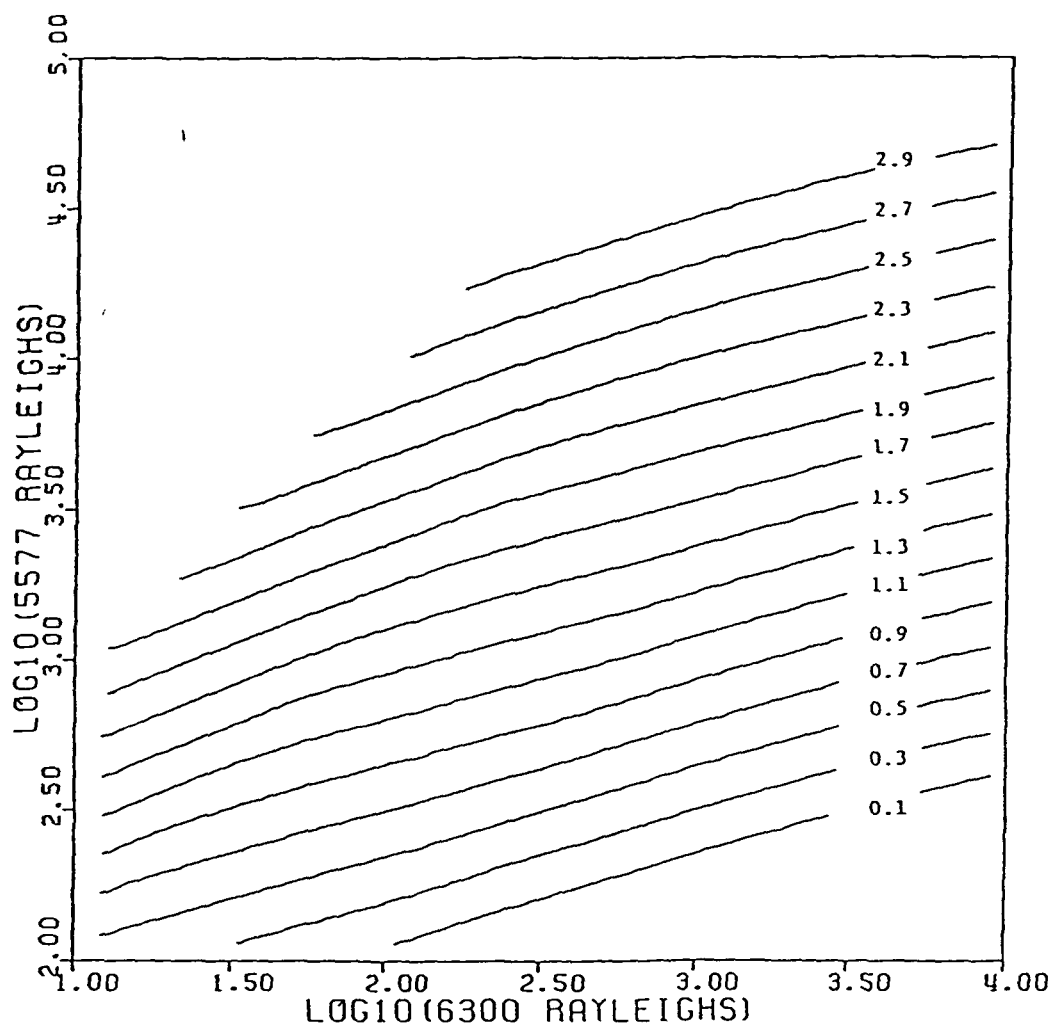
Figure 1. Contours of $\log_{10}$ energy flux as a function of the 5577 and 6300 Å intensities. The energy flux is in units of ergs/(cm^{2}s).

Figure 2   Left panel shows the DE-2 orbit track crossing the SAI image. In the right panel the logarithm of the auroral energy flux along this track is shown. Three sources of energy flux are used; SAI image, LAPI DE-2 observation, and Spiro et al. [1982] model.

DE-2 SATELLITE MEASUREMENT

COMPUTED FROM DIGITIZED IMAGES

MODEL (SPIRO ET AL, 1982)

LOG SEFLUX

DE-2 SATELLITE
ORBITAL PATH

12 MLT
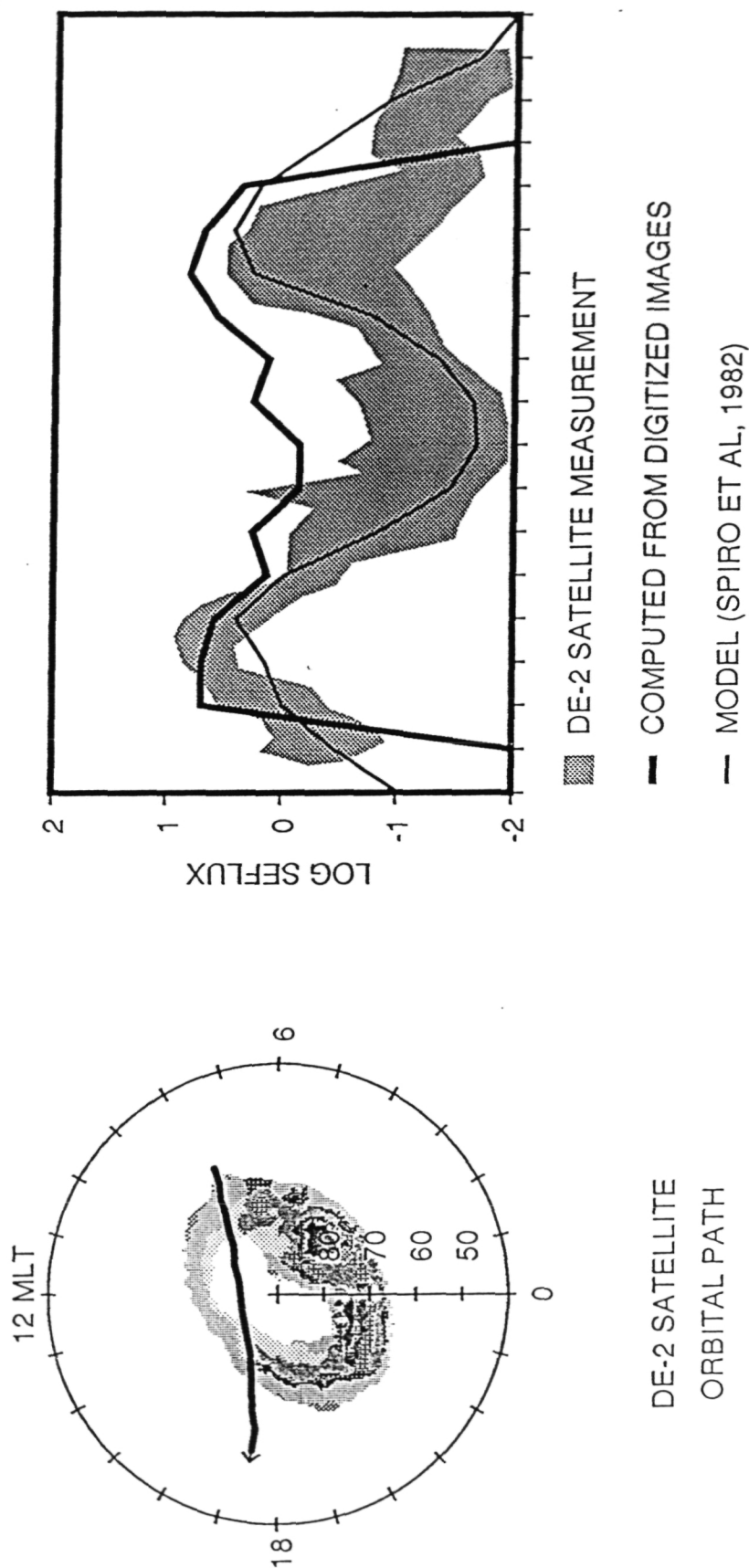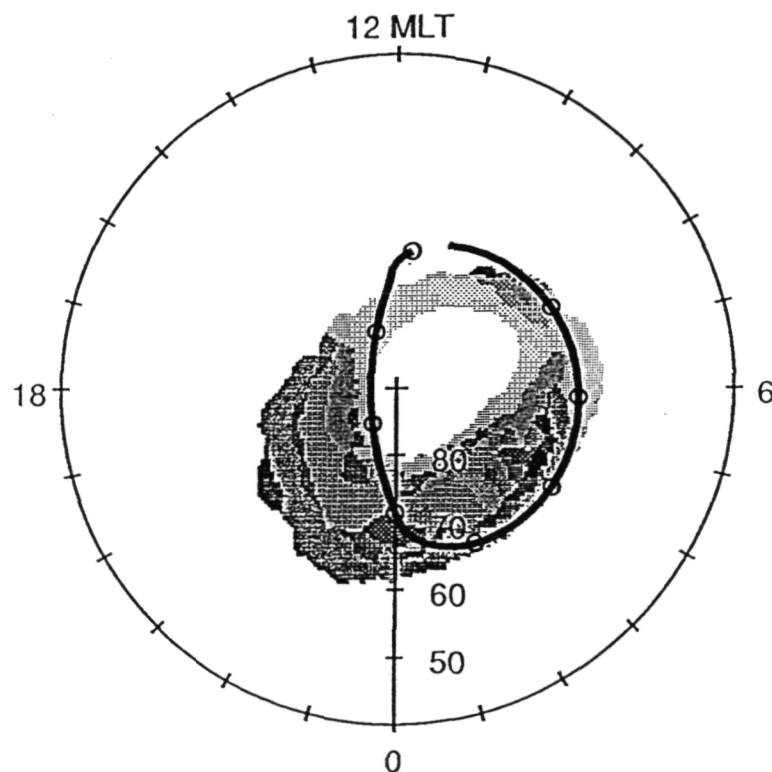
Figure 3. Grey scaled auroral energy flux for the image at 0410 UT. Darkest shades correspond to highest energy fluxes. The test trajectory is shown as a bold line, the circles are drawn every 10th profile storage step around the trajectory.
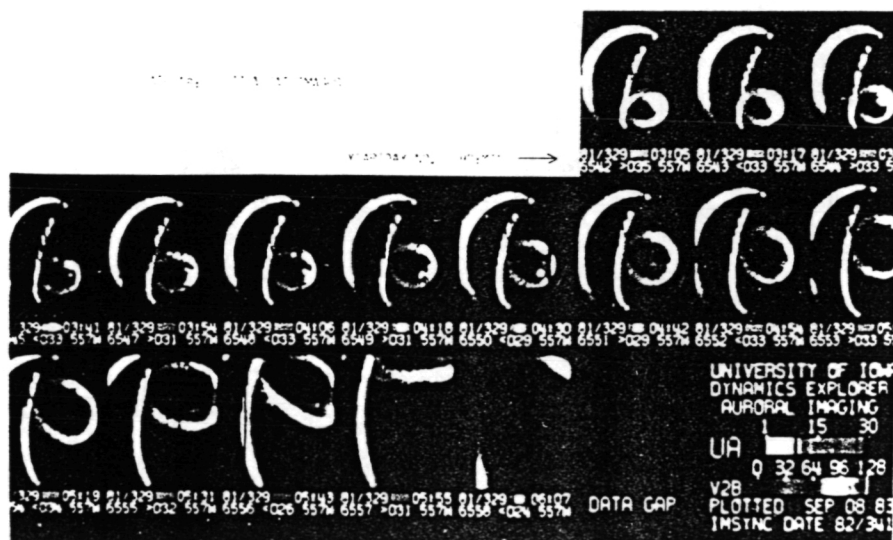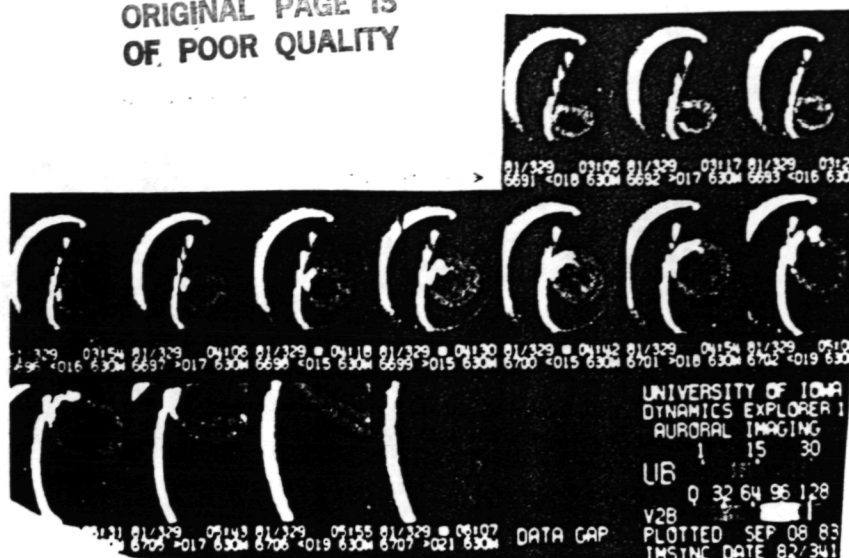
Plate 1. Two simultaneous auroral image sequences from DE-1, SAI on Day 329, 1981. The first image began at 0305 UT and continued through to 0607 UT. Top panel shows 6300 Å while the bottom panel is for 5577 Å.
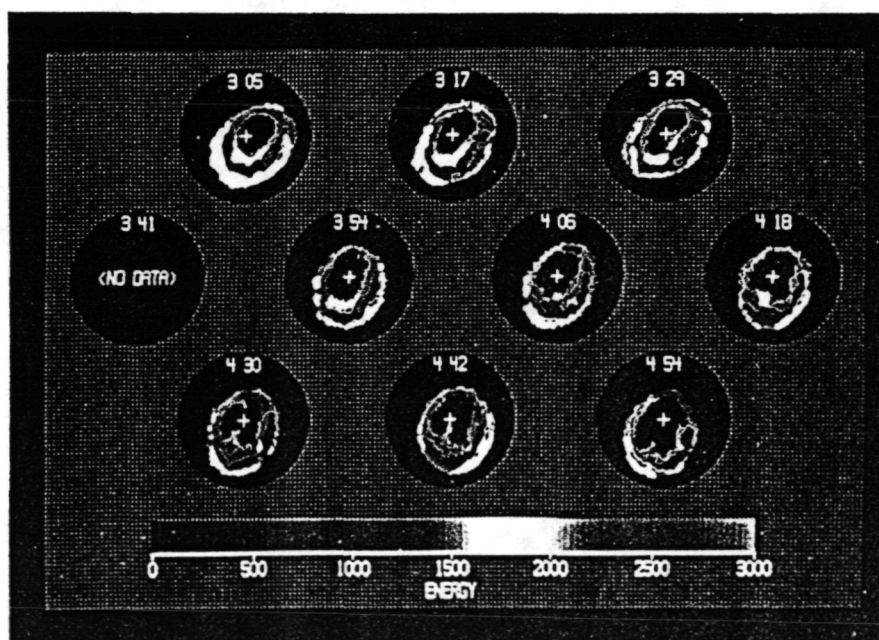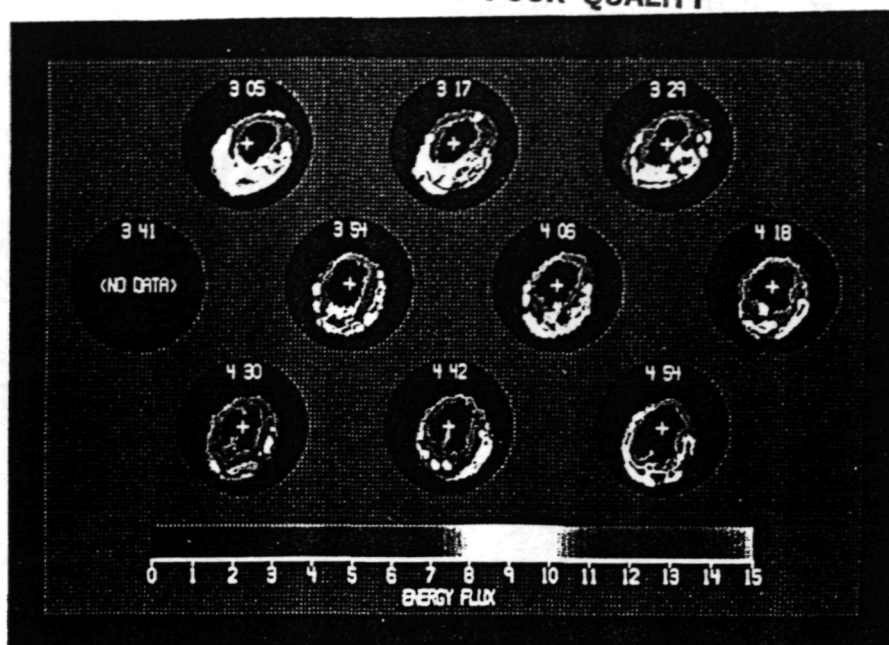
Plate 2. Auroral energy flux (top panel) and characteristic energy (bottom panel), for part of the SAI image sequence shown in Plate 1. Dials correspond to MLT - magnetic latitude polar plots extending poleward from 50°. Noon is at the top and dawn on the right side of each dial. The energy flux is in units of erg cm^{-3} s^{-1} and the energy in eV. Each dial is identified with its UT time in HR:MIN.
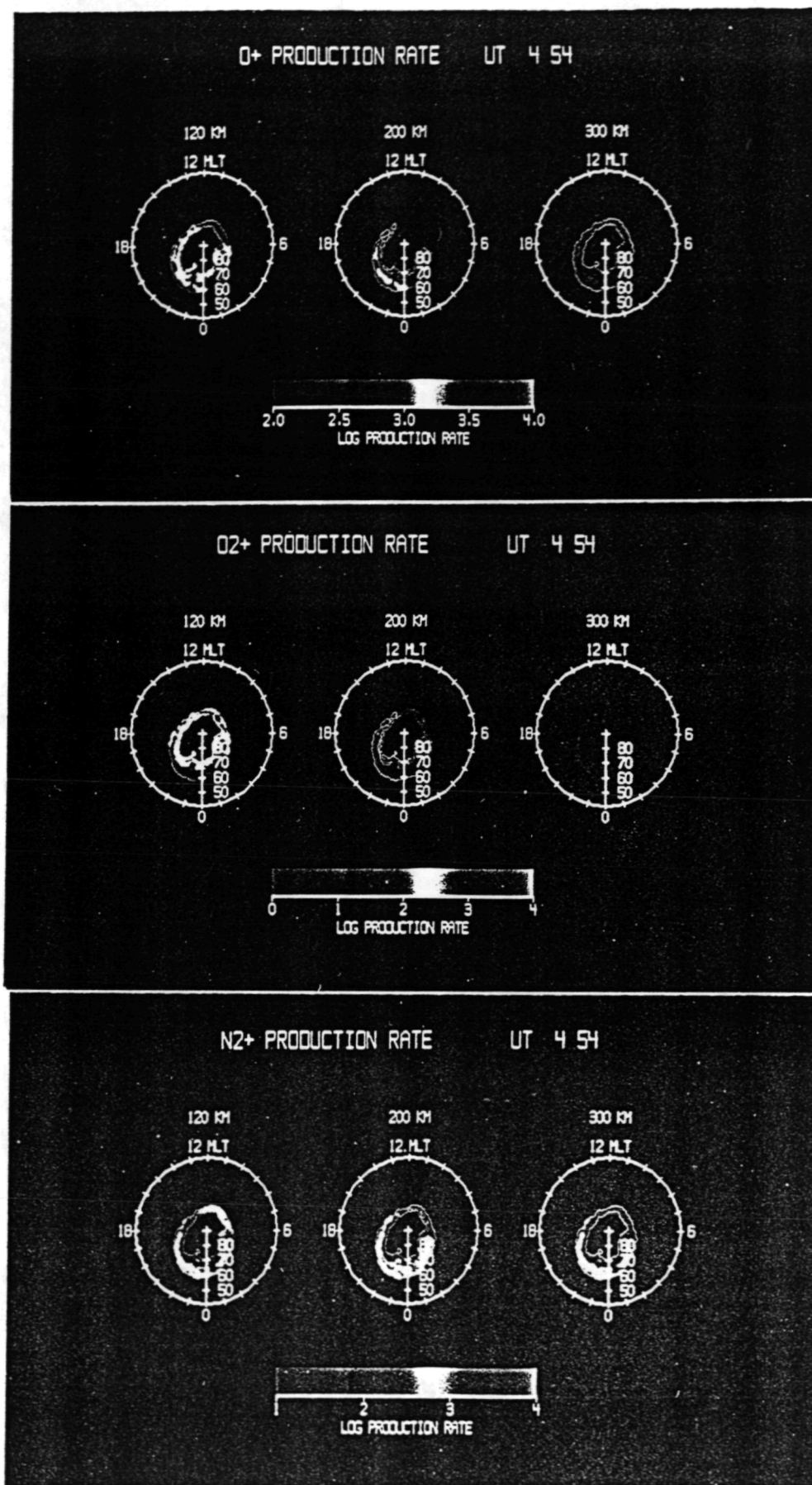
Plate 3. Ionization rates at three altitudes for O^+ (top panel), O_2^+ (middle panel), and N_2^+ (bottom panel). The dials are MLT - magnetic latitude, and the production rates are in ions $cm^{-3} s^{-1}$. Note the dynamic range used in each panel is different.
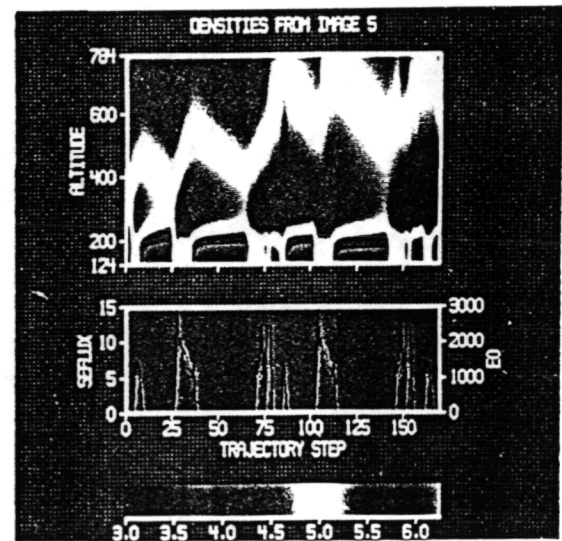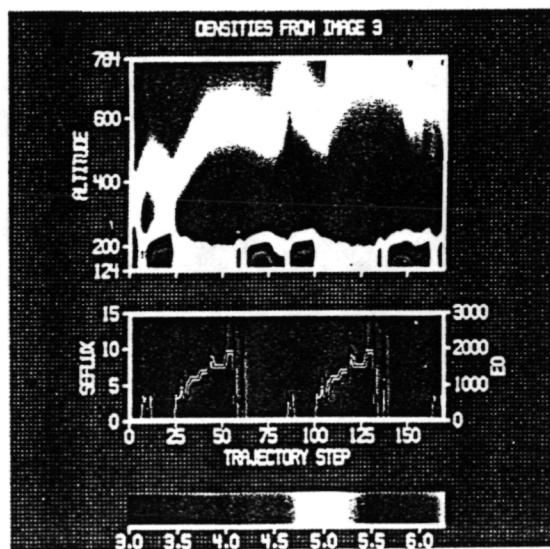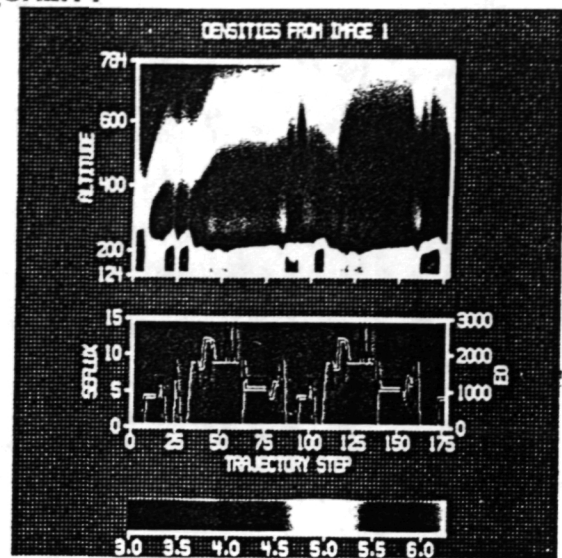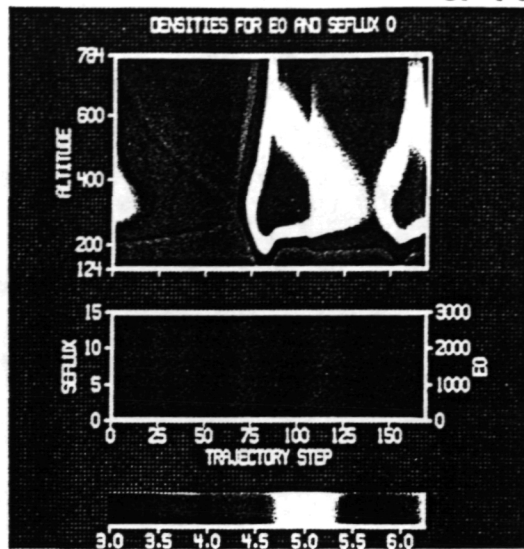
Plate 4. TDIM trajectory runs for various auroral configurations. In each set of panels the electron density is color coded as a function of altitude and position along the trajectory. The sub-panel beneath this shows the energy flux (SEFLUX) black line and characteristic energy (EO) red line variations along the trajectory. Panel a (top left) is for zero auroral precipitation and shows the solar EUV variations. Panel b (top right) is for 0305 UT; Panel c (bottom left) is for 0442 UT; and Panel d (bottom right) is for 0329 UT.